



Originally published as:

*Bloßfeld M., Seitz M., Angermann D., Moreaux G. (2016) **Quality assessment of IDS contribution to ITRF2014 performed by DGFI-TUM.** Advances in Space Research, published online*

DOI: [10.1016.j.asr.2015.12.016](https://doi.org/10.1016/j.asr.2015.12.016)

Accepted by Advances in Space Research after review process.

Quality assessment of IDS contribution to ITRF2014 performed by DGFI-TUM

Mathis Bloßfeld^{a,*}, Manuela Seitz^a, Detlef Angermann^a, Guilhem Moreaux^b

^a*Deutsches Geodätisches Forschungsinstitut der Technischen Universität München (DGFI-TUM)
Arcisstraße 21, 80333 Munich, Germany*

^b*Collecte Localisation Satellites, 8-10 rue Hermès, Parc technologique du Canal, 31520 Ramonville Saint-Agne, France*

Abstract

The International DORIS Service (IDS) submitted input data for the most recent realization of the International Terrestrial Reference System (ITRS), the International Terrestrial Reference Frame 2014 (ITRF2014). As one of the ITRS Combination Centers, DGFI-TUM is in charge to analyze and assess the quality of the submitted data and to compute a combined global TRF solution (called DTRF2014) using observations of the four geodetic space techniques GNSS, VLBI, SLR and DORIS. The combination methodology used at DGFI-TUM is based on the combination of datum-free normal equations. Together with station coordinates and velocities, terrestrial pole coordinates are estimated in one common adjustment. The paper presents the analysis results of the most recent DORIS submission IDS-d09 and evaluates its quality w.r.t. the DTRF2008 (IDS-only) solution. In the most recent version of the analysis, we introduce in total 56 station discontinuities and reduce 15 stations due to a too short time span or too few observations. Time series of weekly IDS solutions are computed and validated w.r.t. DTRF2008. The transformation parameter time series and the station residuals are discussed in detail. Especially the scale parameter time series shows a significant improvement compared to the DTRF2008 input data. The scatter of the x- and y-translation is significantly reduced to 5.7 mm and 7.1 mm compared to 6.6 mm and 8.1 mm for the DTRF2008 (IDS-only) solution. The z-translation time series still shows a high correlation with solar activity. 10 % of all station residuals are significantly affected by spectral peaks at draconitic period harmonics of the altimetry satellites Jason and TOPEX/Poseidon and up to 48 % of all station residual time series contain significantly determined frequencies with a 14 day period. The multi-year IDS solution is validated w.r.t. DTRF2008 and the consistently estimated terrestrial pole coordinates are analyzed and compared to IERS 08 C04. The x-pole spectra comprises prominent peaks at various draconitic frequencies.

Keywords: IDS, DORIS, ITRF2014, DTRF2014, Terrestrial Reference Frame, Polar Motion

1. Introduction

The official realization of the International Terrestrial Reference System (ITRS) is computed every three to five years. The computation of the International Terrestrial Reference Frame 2014 (ITRF2014) is based on the combination of observations of the four geodetic space techniques Global Navigation Satellite Systems (GNSS), Very Long Baseline Interferometry (VLBI), Satellite Laser Ranging (SLR) and Doppler Orbitography and Radiopositioning Integrated by Satellite (DORIS). As one of three ITRS Combination Centers of the International Earth Rotation and Reference Systems Service (IERS), DGFI-TUM is computing an ITRS realization through combination of the four techniques at the normal equation level of the Gauß-Markov model (Seitz et al., 2012; Bloßfeld, 2015). This realization is called DGFI-TUM Terrestrial Reference Frame 2014 (DTRF2014).

The analysis results presented in this paper are achieved in the framework of the DTRF2014 computation and are

validated w.r.t the previous realization of the DTRF, the DTRF2008 (Seitz et al., 2012). All DTRF realizations are based on the same input data provided for the official ITRF solutions.

Compared to the input data of the International DORIS Service (IDS; Willis et al., 2010) for the DTRF2008 solution (Altamimi and Collilieux, 2010; Angermann et al., 2010; Valette et al., 2010; Seitz et al., 2012), several improvements of the IDS data concerning the space and ground infrastructure and the a priori modeling have been achieved. For a detailed discussion of the improvements, please see Willis et al. (2015); Moreaux et al. (2016). Hereafter, only the most important improvements concerning the infrastructure and the modeling of measurements and satellite perturbations are briefly discussed.

The space segment improved significantly due to the launch of four new DORIS-tracked satellites, namely Jason-2, CryoSat-2, HY-2A and SARAL (Satellite with ARGOS and ALtika). In the same period, the DORIS tracking of three old satellites called SPOT-2 (Satellite Pour l'Observation de la Terre), SPOT-4 and Envisat (Environmental satellite) was stopped. The new satellites carry

*Corresponding author

Email address: mathis.blossfeld@tum.de (Mathis Bloßfeld)

new generation receivers, so called DGXX receivers, on-board which allow to track up to seven beacon signals in parallel. The ground station network also improved. Compared to DTRF2008, four new beacons have been installed at Cold Bay (USA), Grasse (France), Betio Island (Kiribati) and Rikitea (French Polynesia) and the global station distribution was further homogenized (in terms of global distribution, beacon models and antenna base types; [Moreaux et al., 2016](#)). Besides the improvement of the infrastructure, also the modeling of the DORIS measurements and force model effects was improved. The DORIS measurements now take into account (a) beacon frequency variations, (b) phase law and (c) South Atlantic Anomaly (SAA) effects on Jason-1 and SPOT-5 ([Štěpánek et al., 2014](#)). In addition to the improved measurement modeling, time variable gravity fields (e.g., EIGEN-6S2, [Rudenko et al., 2014](#)) are now used in the analysis. The improvement of the non-conservative force models for solar radiation pressure and air drag have to be handled with care since various DORIS Analysis Centers (ACs) assert that they have improved the satellite non-conservative force modeling in different ways (e.g., [Soudarin et al., 2016](#); [Lemoine et al., 2016](#)). This fact might lead to inconsistencies in the DORIS-only combination. Furthermore, tracking data of SPOT-4 and Envisat have been corrected ([Moreaux et al., 2016](#)).

The first part of this paper deals with the analysis of the submitted IDS SINEX (Solution INdependent EXchange format) files and quantities such as the reconstructed squared sum of the residuals and the individual weighting of the AC solutions are validated. SINEX files contain values of estimated parameters (usually station positions and velocities or Earth Orientation Parameters) as well as the full covariance matrix associated with these parameters. In addition, changes of the satellite constellation and ground station distribution are described. Sect. 3 presents a brief description of the TRF computation approach at normal equation level used at DGFI-TUM. The explained algorithm is then used to compute weekly and multi-year IDS-only Terrestrial Reference Frames (TRFs). Furthermore, it is used to compile a list of the introduced discontinuities and reduced stations. Sect. 4 provides some major results of the DORIS data analysis and includes also a quality assessment of the computed weekly IDS solutions and the multi-year IDS solution. Finally, Sect. 5 summarizes the presented results and gives an outlook.

2. DORIS data / IDS submissions

IDS SINEX files

The Combination Center (CC) of the International DORIS Service (IDS) made available in total 1141 weekly SINEX files which cover a conventional time span between 03.01.1993 and 28.12.2014 to the IERS Data Center (DC). The submitted data were obtained by combining solutions of up to six different IDS-ACs, namely ESA (Germany),

GOP (Czech Republic), GSC (USA), IGN (France), INA (Russia) and LCA/GRG (France). The IDS-ACs use five different software packages and therefore lower the possibility of systematic software-dependent errors in the combined IDS solution. Only 6 weekly SINEX files were missing due to (a) only a few ACs available during the weeks, (b) due to bad data quality and (c) due to poor position quality ([Moreaux et al., 2016](#)). All SINEX files contain weekly 3-dimensional station coordinate solutions at mid-week epochs with consistently estimated daily terrestrial pole coordinates at noon epochs which are slightly stabilized by minimum constraints. Due to the fact that solutions are stored in the SINEX files and no a priori coordinates are given, the estimated coordinates are assumed to be equal to the respective a priori coordinates. The time interval beginning at 1993.0 was chosen by the IDS since during this time period, at least two satellites are tracked simultaneously and the DORIS station network was completed in August 1992 ([Moreaux et al., 2016](#)). The statistical information stored in the IDS SINEX files contain the number of observations n , the number of unknowns u , the redundancy (degree of freedom) r and the a posteriori matrix scaling factor $\hat{\sigma}_0^2$. Since the stochastic model for the combination at normal equation level needs the squared sum of the observed minus computed values $\mathbf{l}^T \mathbf{P} \mathbf{l}$ and residuals $\hat{\mathbf{v}}^T \mathbf{P} \hat{\mathbf{v}}$ for each individual matrix, they are reconstructed using the following equation:

$$\mathbf{l}^T \mathbf{P} \mathbf{l} = \hat{\mathbf{v}}^T \mathbf{P} \hat{\mathbf{v}} = r \cdot \hat{\sigma}_0^2 \quad (1)$$

with the vector of observed minus computed with a priori values \mathbf{l} , the vector of residuals $\hat{\mathbf{v}}$ and the weight matrix of the observations \mathbf{P} . A prerequisite for this construction of the stochastic model is the fact that the estimated parameters are equal to the a priori values. Fig. 1 shows the weekly $\hat{\mathbf{v}}^T \mathbf{P} \hat{\mathbf{v}}$ values reconstructed using Eq. 1 for the most recent IDS submission (d09). Systematic changes in the $\hat{\mathbf{v}}^T \mathbf{P} \hat{\mathbf{v}}$ time series are mainly caused by changes in the satellite constellation. Especially, since GPS week 1798 (June 22nd, 2014), the small $\hat{\mathbf{v}}^T \mathbf{P} \hat{\mathbf{v}}$ values might be caused by the inclusion of the SARAL satellite. This fact has to be further investigated.

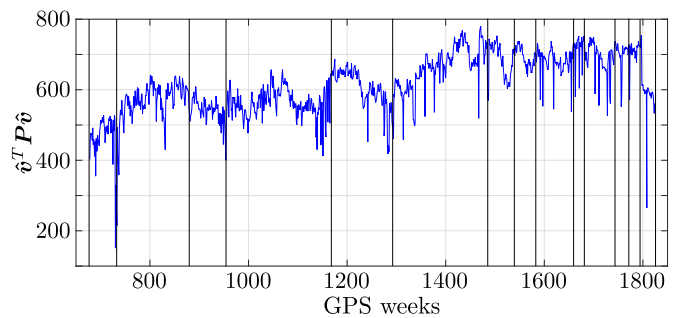


Figure 1: Reconstructed weekly squared sums of residuals $\hat{\mathbf{v}}^T \mathbf{P} \hat{\mathbf{v}}$ for the IDS submission d09 between GPS week 678 (1993.0) and 1824 (2015.0).

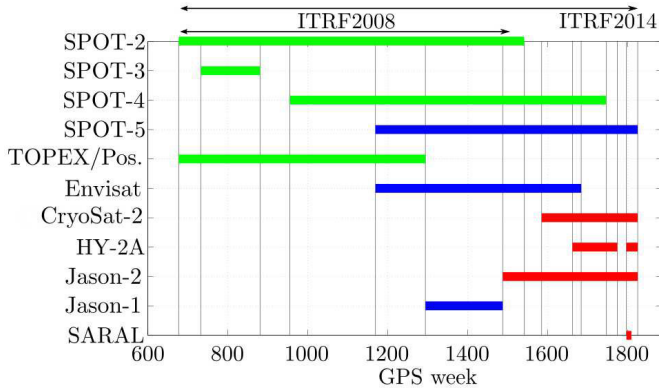


Figure 2: DORIS tracked satellite constellation between GPS week 678 (1993.0) and 1824 (2015.0). The green bars indicate satellite observations using first generation DORIS receivers, the blue bars indicate satellites with second generation DORIS receivers and the red bars indicate satellites with new so-called DGXX receivers. For ITRF2008, only observations of the first two receiver types has been used (green + blue bars) whereas for ITRF2014, observations of all receivers are used (green + blue + red bars).

Satellite constellation

The IDS data for ITRF2014 contains observations to 11 satellites, namely SPOT-2, SPOT-3, SPOT-4, SPOT-5, TOPEX/Poseidon (named after the ocean TOPography EXperiment and the Greek god of the ocean Poseidon), Envisat, CryoSat-2, HY-2A, Jason-1, Jason-2 and SARAL, between 1993.0 and 2015.0. Within this conventional time interval, at least two and at most six satellites have been observed in parallel and in total, 15 changes in the DORIS-tracked satellite constellation occurred. They are shown in most of the following figures as vertical gray lines. In the most recent years, the number of changes increased due to various recently launched satellites and the end of former satellite missions. The question of how the changes of the constellation affect the geodetic parameter time series is discussed in Sect. 4. The information about the included satellites can be extracted from an extended comment block of the IDS SINEX files. Fig. 2 shows the DORIS-tracked satellite constellation used for the ITRF2014 computation. It has to be mentioned here that the inclusion of the missions Jason-1, HY-2A and SARAL was optional for the individual ACs. Therefore, Jason-1 and SARAL have been included by three ACs (Jason-1: ESA, GRG, GSC; SARAL: GRG and IGN) whereas HY-2A was included only by ESA, GRG, GSC and IGN (Moreaux et al., 2016). Three different types of on-board DORIS receivers have to be distinguished (see Tab. 1). The first generation DORIS receiver (1G) can record only one DORIS signal at the same time (green bars in Fig. 2). Satellites with first generation receivers are SPOT-2, SPOT-3, SPOT-4 and TOPEX/Poseidon (Moreaux et al., 2016). The second receiver generation (2G/2GM) can record two DORIS signals in parallel (blue bars in Fig. 2; SPOT-5, Envisat, Jason-1). The newest type of DORIS receivers, the so-called DGXX receivers (CryoSat-2, HY-2A, Jason-

2, SARAL) are shown as red bars in Fig. 2 and can process signals from up to seven beacons at the same time. Therefore, much more observations are recorded compared to the first generation DORIS receivers. As an example, Moreaux et al. (2016) stated that the number of observations of Jason-2 during one week is comparable to the set of all observations from the Envisat, Jason-1, SPOT-4 and SPOT-5 missions. In addition to the receiver types, Tab. 1 summarizes the draconitic periods of the satellites. Except the Jason-1/2, TOPEX/Poseidon and CryoSat-2 draconitic periods, the values of the sun-synchronous satellites are close to infinity (at least multiple years) since the nodal period (time period when the secular nodal precession $\dot{\Omega}_{\text{sec}}$ completes 360°) is nearly equal to the annual period. This means, that a mismodeling of the solar radiation pressure for these satellites can also cause errors at annual periods (see also Valette et al., 2010; Gobinddass, 2009).

Table 1: Characteristics of satellites included in ITRF2014 IDS submission. The mean orbital elements for the satellites are taken from http://cddis.nasa.gov/sp3c_satlist.html.

satellite	rec. type	altitude/ inclination [km]/[$^\circ$]	nodal period [days]	draconitic period [days]
SPOT-2	1G	≈ 786 98.7°	358.75	20142
SPOT-3	1G	≈ 832 98.7	366.87	82634
SPOT-4	1G	≈ 802 98.7	361.56	35756
TOPEX/ Poseidon	1G	≈ 1350 66.0	-173.94	117.83
Envisat	2G	≈ 800 98.0	392.58	5247.3
SPOT-5	2GM	≈ 777 98.7	357.17	16145
Jason-1	2GM	≈ 1336 66.0	-172.84	117.32
CryoSat-2	DGXX	≈ 720 92.0	1505.31	482.27
HY-2A	DGXX	≈ 971 99.35	365.18	< 99999
Jason-2	DGXX	≈ 1336 66.0	-172.84	117.32
SARAL	DGXX	≈ 814 98.55	370.01	28406

Datum information of SINEX solutions

The submitted IDS SINEX files contain solutions with a fixed geodetic datum. This means, the reconstructed normal equations will not contain any singularities w.r.t. the origin, the orientation and the scale. Fig. 3 shows the mean formal errors of the datum information stored in the SINEX files. The procedure how to derive these formal errors is presented in detail by Sillard and Boucher

(2001). The formal errors of all datum components are below $2 \cdot 10^{-3}$ mm and decrease with time. This decrease can be explained with the larger satellite constellation in the most recent years and the increase of observations due to new receiver types.

Since the minimum constraints, which are used for the datum definition of the weekly IDS solutions, are not booked in the IDS SINEX files, similarity transformation parameters have to be introduced in order to create datum-free normal equations (see Bloßfeld, 2015). Datum-free normal equations (NEQs) have to be reconstructed since the combination algorithm of the DGFI-TUM ITRS CC is based on the normal equation level of the Gauß-Markov model (Seitz et al., 2012; Bloßfeld, 2015). Datum-free NEQs are important for this combination approach in order to avoid any deformation of the combined solution (Bloßfeld, 2015). In total, seven similarity transformation parameters, namely three translation, three rotation and one scale parameter are introduced each week.

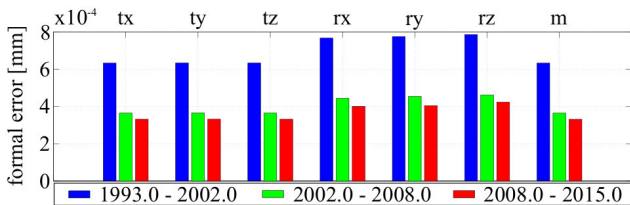


Figure 3: Mean formal errors of weekly datum parameters according to a datum test based on decomposition of the variance-covariance matrices described by Sillard and Boucher (2001) between GPS week 678 (1993.0) and 1824 (2015.0). The rotation and scale formal errors are projected onto the Earth’s crust using $R = 6378137.0$ m.

Weighting of individual IDS-AC solutions

Fig. 4 shows the weekly variance factors σ^2 between GPS week 678 (1993.0) and 1824 (2015.0) of each individual IDS-AC for the IDS-d09 submission. The time series show for all ACs a significant jump in 2008.0 which does not coincide with any change in the satellite constellation. Therefore, the reason for this effect is not yet clear. An example for an effect in the AC weights which coincides with a constellation change is GPS week 1663 (20.11.2011) when the HY-2A satellite is included in the IDS combination.

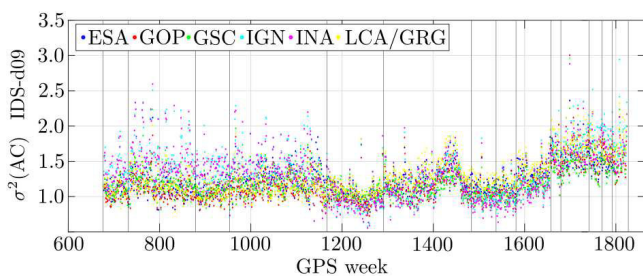


Figure 4: Weekly variance factors σ^2 of individual ACs between GPS week 678 (1993.0) and 1824 (2015.0).

IDS ground station network

The global distribution of the IDS ground station network is shown in Fig. 5. In total, 160 beacons at 71 different stations are distributed nearly homogeneously over the world: 38 sites are located on the northern hemisphere and 33 sites are located on the southern hemisphere (Moreaux et al., 2016). Compared to the DTRF2008 (IDS-only) network, four new sites and one new beacon have been included in the TRF solution. Two of them, namely Betio Island (Kiribati) and Rikitea (French Polynesia) started DORIS observations in 2006.

These stations have not been included in the previous DTRF2008 solution due to a too short time span of observations. Grasse (France) and Cold Bay (USA) started DORIS observations after the DTRF2008 period in 2008 and 2010. The IDS beacon SOEB at the station Socorro Island (Mexico) has operated since April 25th, 2014. The beacons SODA and SODB, which are closely located to SOEB, are already included in the DTRF2008 solution but not in the ITRF2008 solution. In addition to the IDS stations, also the core station network used for the datum definition of the IDS part of the DTRF2008 and DTRF2014 is shown in Fig. 5. The stations are selected on the basis of a long and stable observation time series and a homogeneous global distribution. For the DTRF2014 (IDS-only) solution, in total 59 datum stations have been defined. The histograms in Fig. 5 emphasize that one of the strengths of the DORIS technique is the homogeneous station distribution and the large number of stations on the southern hemisphere (101 beacons at 38 sites compared to 31 sites of DTRF2008). The rationale of this nearly optimal global coverage of DORIS beacons was so that there should always be a station in view of the SPOT-2 satellite at about 832 km altitude (Fagard, 2006).

3. Accumulation of time series

Methodology

In this section, the computation approach of the DTRF2014 is presented. As input data, the official IDS submissions for the ITRF2014 are used. Fig. 6 describes the methodology applied at DGFI-TUM to compute the IDS-only multi-year TRF solution. The weekly SINEX files, submitted by the IDS, are tested for completeness. The geodetic datum of each file is analyzed in order to detect possible inconsistencies in the IDS solution time series. Afterwards, datum-free NEQs are reconstructed by introducing seven similarity transformation parameters each week (see Bloßfeld, 2015). The weekly datum-free NEQs are then used for the computation of weekly TRF+EOP solutions (Terrestrial Reference Frame + Earth Orientation Parameters). To compute the solutions, the geodetic datum is realized each week by applying a no-net-translation (NNT), a no-net-rotation (NNR) and a no-net-scale (NNS) condition on the selected datum station network shown in Fig. 5 w.r.t. its a priori values (equal to the position estimates in the IDS SINEX files; see Sect. 2).

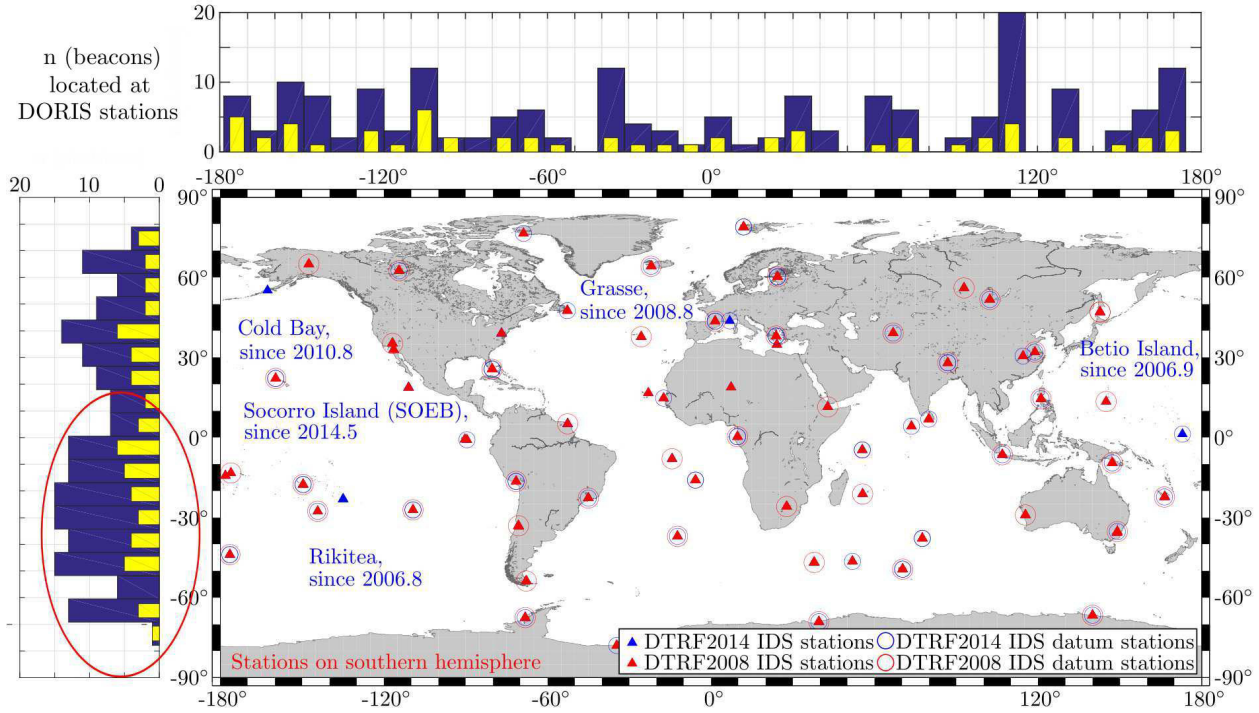


Figure 5: DORIS beacon ground network of IDS contribution of DTRF2008 (red triangles) and DTRF2014 (blue + red triangles). The datum stations of the IDS-only multi-year solution of the DTRF2008 and DTRF2014 are shown as red and blue circles, respectively. In addition, the histograms of the DTRF2014 beacons (blue bars) and of the DTRF2014 (IDS-only) datum beacons (yellow bars) located at DORIS stations (blue + red triangles) w.r.t. latitude and longitude are shown.

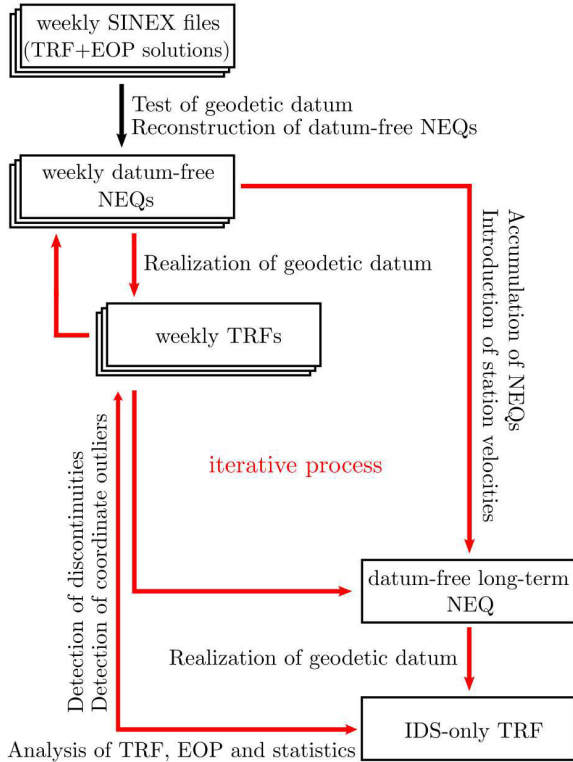


Figure 6: Schematic view of accumulation methodology applied at DGFI-TUM.

The selection of datum station is based on the stability and length of station time series and, in addition, on the global distribution. The time series of TRF+EOP solutions are used to detect coordinate outliers ($3 - \sigma$ criteria for station residuals) and discontinuities in the station coordinate time series. Therefore, each station position time series is analyzed for significant offsets or drift changes in any component. In some cases, no reason for the offset/drift change can be found (see top-right column in Tab. 2). Afterwards, the outliers are reduced and the discontinuities are applied to the weekly datum-free NEQs. The application of the discontinuities is realized in such a way that a new set of coordinates (and velocities) is estimated and the solution number of the corresponding station is increased (see column 4 in Tab. 2). The station motion is parametrized through linear velocities. Non-linear post-seismic relaxation motions for stations such as Arequipa, Santiago and Fairbanks (stations which might be most affected by recent big earthquakes) are approximated by a piece-wise linear station motion model. The modified NEQs are accumulated and common parameters like station coordinates and velocities are stacked. The result is a datum-free long-term NEQ. After the geodetic datum is realized (by applying NNT, NNR and NNS conditions on the datum station coordinates and velocities w.r.t. DTRF2008), the IDS-only multi-year reference frame is computed by inverting the accumulated and constrained NEQ. This solution contains station coordinates and velocities as well as daily offsets

Table 2: 56 introduced station coordinate discontinuities of the DTRF2014 IDS-only solution.

IDS name	DOMES number	discontinuity epoch [yy:ddd]	new solution number	description
ADEA	91501S001	98:084	0A02	Earthquake Mw 8.1
ADGB	61501S004	14:161	0A02	Beacon change
ASDB	30602S004	05:014	0A02	Unknown reason
ASDB	30602S004	07:171	0A03	Unknown reason
CADB	41609S002	08:183	0A02	Beacon change
CADB	41609S002	11:355	0A03	Unknown reason
CHAB	50207S001	06:340	0A02	Antenna phase bias
CICB	23101S002	06:049	0A02	Drift change in H
COLA	23501S001	94:320	0A02	Earthquake
EASB	41703S009	08:196	0A02	Discontinuity in N
EASB	41703S009	11:186	0A03	Beacon change
EASB	41703S009	12:340	0A04	sign. jump in N
EVEB	21501S001	02:075	0A02	Unknown reason
EVEB	21501S001	11:261	0A03	Earthquake
FAIB	40408S005	02:307	0A02	Earthquake
FAIB	40408S005	03:033	0A03	Post seismic
FAIB	40408S005	03:215	0A04	Post seismic
FAIB	40408S005	06:001	0A05	Post seismic
GOMB	40405S037	04:143	0A02	Unknown reason
GREB	40451S176	06:025	0A02	Unknown reason
HELB	30606S003	00:035	0A02	Antenna tilt
HEMB	30606S004	08:209	0A02	Earthquake
KESB	91201S004	04:036	0A02	Unknown reason
KRUB	97301S004	97:001	0A02	Discontinuity
KRUB	97301S004	05:117	0A03	Discontinuity
LICB	32809S004	08:215	0A02	Unknown reason
MAHB	39801S005	09:089	0A02	Beacon change
MANB	22006S002	12:168	0A02	Earthquake
MARB	30313S002	02:167	0A02	Earthquake
MATB	30313S003	06:311	0A02	Antenna offset
PDMB	31906S002	08:160	0A02	USO change
REUB	97401S002	08:210	0A02	Unknown reason
REYB	10202S002	00:169	0A02	Earthquake
REZB	10202S003	05:073	0A02	Discontinuity E/N
REZB	10202S003	08:157	0A03	Unknown reason
REZB	10202S003	12:136	0A04	Beacon change
RIPB	41507S005	05:154	0A02	Unknown reason
ROTA	66007S001	02:013	0A02	Unknown reason
SAKA	12329S001	94:282	0A02	Earthquake
SAKA	12329S001	98:360	0A03	Unknown reason
SALB	39601S002	08:117	0A02	Jump in N
SANB	41705S009	05:327	0A02	Earthquake
SANB	41705S009	08:197	0A03	Unknown reason
SANB	41705S009	10:058	0A04	Chile Earthquake
SANB	41705S009	11:045	0A05	Earthquake
SODA	40503S003	-95:360	0A02	Volcanic activity
SODA	40503S003	97:149	0A03	Volcanic activity
SODB	40503S004	02:276	0A02	Unknown reason
SPJB	10317S005	04:347	0A02	after data gap
STJB	40101S002	02:230	0A02	Unknown reason
SYPB	66006S003	08:194	0A02	Unknown reason
SYPB	66006S003	12:193	0A03	Unknown reason
THUB	43001S005	06:127	0A02	Unknown reason
TLSB	10003S005	12:301	0A02	Unknown reason
TRIA	30604S001	99:198	0A02	Unknown reason
TRIB	30604S002	04:228	0A02	Unknown reason

of terrestrial pole coordinates. The estimation of weekly TRF solutions, the detection of discontinuities and outliers and the computation of the IDS multi-year solution are iteratively done (see red arrows in Fig. 6) in order to keep the number of outliers and discontinuities as small as possible.

Station discontinuities

All introduced station discontinuities are summarized in Tab. 2. In total, 56 discontinuities have been defined (compared to 48 in DTRF2008; Seitz et al., 2012) which were iteratively determined together with the IDS CC. This means, that the weekly IDS-only solutions contain coordinates of $160 + 56 = 216$ coordinate and velocity sets for 160 beacons. For most of the discontinuities, explicit reasons for an abrupt motion or change of the long-term drift could be found. Nevertheless, some discontinuities can still not be explained by geophysical or technical reasons. The selection and introduction of the discontinuities is, to a certain extent, analyst-dependent. Therefore, a special effort must be made to ensure that all ITRS CCs develop and use the same unique list of discontinuities. This harmonization is currently still missing which means that Tab. 2 might change after the publication of this manuscript.

Reduced stations

In order to estimate reliable and stable station velocities, stations must observe at least 2.5 years in total. Velocity estimates which are based on shorter time intervals are significantly affected by annual signals (Blewitt and Lavallée, 2002). In order to retain stations of interest in the estimated TRF, the time span is decreased to 1.5 years. In addition, a threshold of at least 10 contributing weeks for each station is applied for the estimated TRF. Tab. 3 summarizes the 15 reduced stations which are not included in the IDS part of the DTRF2014. Despite the above mentioned criteria, the DORIS beacon 40101S003 (St. John’s, Canada, STKB) is still included although STKB observed only 50 weeks in 2014. This is done in order to keep the computed DTRF as up-to-date as possible. STKB is not marked as new station in Fig. 5, since STJB (Starec antenna) is already operating since the middle of 1999. Since 15 stations are reduced, the DTRF2014 (IDS-only) solution contains in total coordinates of 200 different position and velocity sets.

4. Results

4.1. Time series analysis

After the computation of the weekly IDS solutions (IDS-only epoch reference frames), weekly 7-parameter similarity transformations w.r.t. the combined DTRF2008 solution are computed in order to identify possible discontinuities and outliers in the station position time series. For the weekly transformations, the same subnet as for the weekly and long-term datum realization is used (see Sect. 3).

Table 3: 15 reduced stations of IDS submission.

IDS name	DOMES number	solution number	# weekly pos estimates	data span
GR4B	10002S019	0A01	18	140
REZB	10202S003	0A01	24	200
SPJB	10317S005	0A01	19	150
MAUB	30313S005	0A01	1	7
HELB	30606S003	0A02	32	217
GOMB	40405S037	0A02	7	49
FAIB	40408S005	0A02	7	49
FAIB	40408S005	0A03	26	185
SODA	40503S003	0A03	15	108
SOEB	40503S005	0A01	12	90
SANB	41705S009	0A04	45	308
MOSB	51001S003	0A01	15	110
SYQB	66006S005	0A01	12	90
BELB	66018S001	0A01	8	60
NOUB	92701S002	0A01	30	225

Fig. 7 displays the translation parameter time series for the submitted IDS-d09 and the DTRF2008 (IDS-only) solution. Whereas the x-component contains no long-term trend and mostly an annual oscillation, the y-component comprises a long-term drift w.r.t. the DTRF2008 solution in the intervals 1993.0 until 1998.4 (inclusion of SPOT-4) and 2008.6 until 2015.0 (inclusion of Jason-2). The annual variation in both components is slightly reduced due to the improved solar pressure modelling of the sun-synchronous satellites (Gobinddass, 2009; Valette et al., 2010). The scatter of the time series is reduced from 6.6 mm and 8.1 mm for the x- and y-translation of the DTRF2008 (IDS-only) solution (Angermann et al., 2010) to 5.7 mm and 7.1 mm for the IDS-d09 solution. The z-component is still highly correlated with the Sunspot number (see also Seitz et al., 2012) which indicates problems with the solar radiation pressure modeling of DORIS-tracked satellites. Another possible problem might be related to the modeling of the atmospheric drag since the Sunspot number primarily influences the atmospheric density. Moreover, second-order ionospheric effects which are more prominent during the solar maximum are currently not included in the DORIS processing and therefore might also impact the z-translation time series (F. G. Lemoine, personal communication). However, the variation became smaller compared to DTRF2008 and the scatter is reduced from 21.8 mm (Angermann et al., 2010) to 17.5 mm. Fig. 8 displays the corresponding spectra of the translation time series for both solutions. The most prominent peaks in the x-translation are at the annual period with amplitudes of 3.4 mm for the DTRF2008 (IDS-only) and about 2.6 mm for the IDS-d09 solution. In the spectra of the y-translation, the IDS-d09 solution shows a slightly smaller annual amplitude than the DTRF2008 (IDS-only) solution (about 3.6 mm). The DTRF2008 (IDS-only) spectra of the

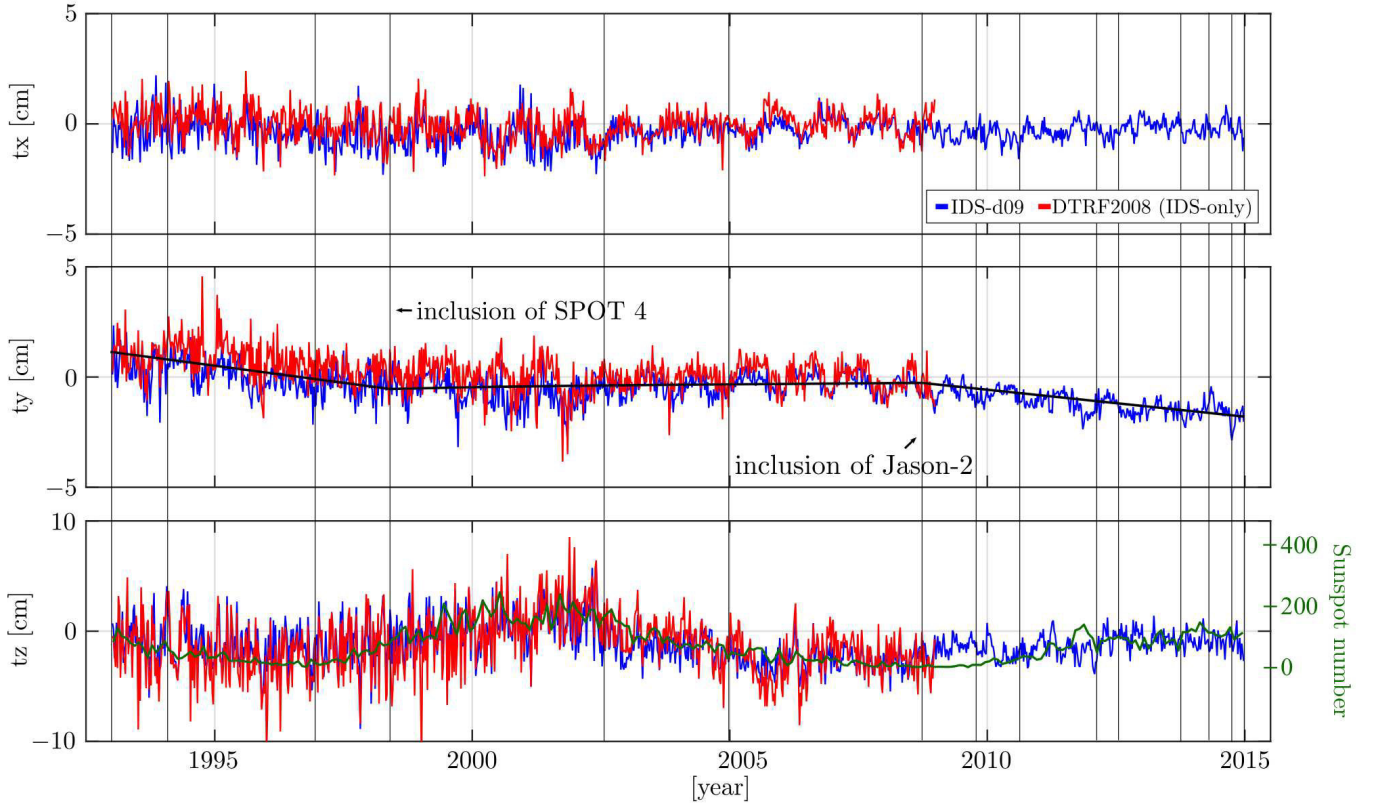


Figure 7: Translation parameter time series in x-, y- and z-direction of weekly IDS-d09 and DTRF2008 (IDS-only) solutions w.r.t. DTRF2008 (combined). In addition to the z-translation, also the Sunspot number (WDC-SILSO, 2015) is plotted.

z-translation shows a lobe and some side lobes near the annual period whereas the IDS-d09 solution contains no prominent peak or side lobes at the annual period. In case of the translations, it can be clearly seen that the quality of the IDS data is improved compared to the DTRF2008 submission since also the scattering of the IDS-d09 time series is significantly reduced.

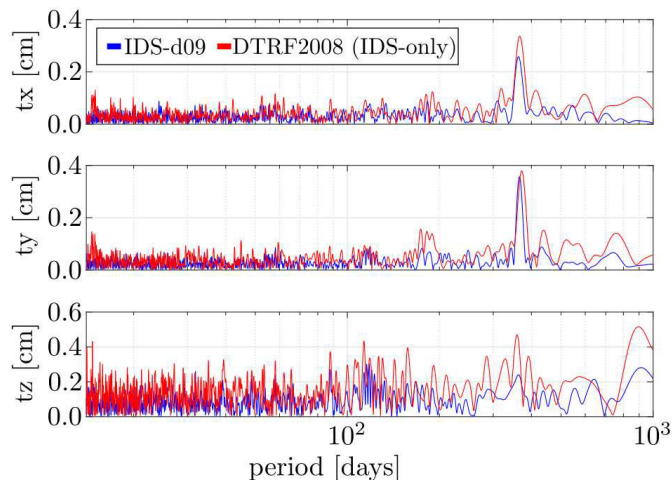


Figure 8: Spectra of the translation parameter time series shown in Fig. 7.

The scale parameter time series and the corresponding spectra are displayed in Fig. 9 and 10. Due to the mentioned improvements in the data analysis applied by the IDS (see Sect. 2 and Moreaux et al., 2016), the scale changes significantly compared to the DTRF2008 (IDS-only) solution. The drift of the DTRF2008 (IDS-only) solution after 2000.0 (about -1.8 mm/yr) is nearly totally removed. Nevertheless, a drift and an offset after 2011.0 still remain in the scale parameter time series. One possible reason might be the inclusion of the HY-2A satellite since November 2011. Moreaux et al. (2016) also expect the inclusion of Jason-2, CryoSat-2 or HY-2A as a possible reason for the scale increase. Between 1994.0 and 1994.2, the scale parameter time series has a significant offset which might be correlated with the exclusion of the the ESA, IGN and INA solutions from the scale combination. INA is excluded throughout the whole time series because they did not apply phase center corrections whereas ESA and IGN are excluded for about 8 weeks when the scale of SPOT-2 was anomalous in early 1994 (Moreaux et al., 2016). This issue needs further investigation. It is also stated by Moreaux et al. (2016), that the ability of all IDS-ACs to estimate beacon frequency offsets already stabilized the IDS scale. The spectra of the scale parameter time series (Fig. 10) comprises significant peaks at 14.7 days (only in the IDS-d09 submission) and 22.36 days (only in the DTRF2008 (IDS-only) solution). The signifi-

cant peak at about 58 days is slightly smaller in the IDS-d09 submission compared to the DTRF2008 (IDS-only) solution. This peak corresponds most likely to a Jason-1/2 or TOPEX/Poseidon draconitic harmonic. However, it is worth to mention here that the Jason/TOPEX tidal alias period for S2 is 59 days and 62 days for M2 (Schlax and Chelton, 1994). Therefore, it might be also possible that a tidal mismodeling or wrong implementation of a tidal model at any AC might cause this systematic (F. G. Lemoine, personal communication). In general, the DTRF2008 (IDS-only) solution scatters more than the most recent IDS-d09 submission.

Additionally, Fig. 9 displays the weekly RMS values of the transformations residuals. Compared to the DTRF2008 (IDS-only) solution, the higher RMS values of the IDS-d09 submission can be explicitly seen before 2002.0 (see also Moreaux et al., 2016). The increased RMS values are still not understood and need further investigation. Even in the transformation of the IDS-d09 weekly solutions on the DTRF2014 IDS-only multi-year solution, the scatter remains higher than in case of DTRF2008. This fact emphasizes that the non-linear station motions are noisier in the IDS-d09 solutions than in the DTRF2008 (IDS-only) solutions due to some unidentified degradation in the IDS modeling, analysis and/or combination. The RMS values increase for the IDS-d09 submission after 2005.0, since the DTRF2008 is extrapolated from 2005.0 and the DTRF2008 only contains observations until 2009.0.

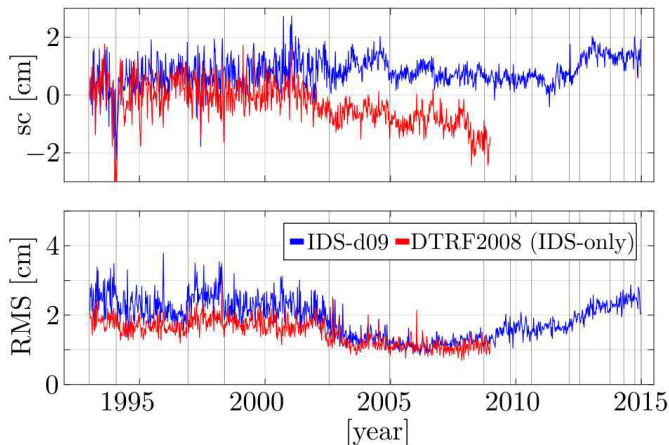


Figure 9: Scale parameter time series and RMS values of the transformations of the IDS-d09 and DTRF2008 (IDS-only) solutions w.r.t. DTRF2008 (combined).

Besides the weekly transformation parameter time series, also the station residuals of the weekly transformations are analyzed. It is planned by the IERS ITRS product center to correct all stations a posteriori for non-tidal atmospheric pressure loading (NT-ATML Altamimi, 2013). Up to now, these mostly annual corrections due to non-tidal atmospheric loading are not applied.

Fig. 11 and 12 exemplarily show the time series and spectra of the DORIS stations Yarragadee (Australia, YASB)

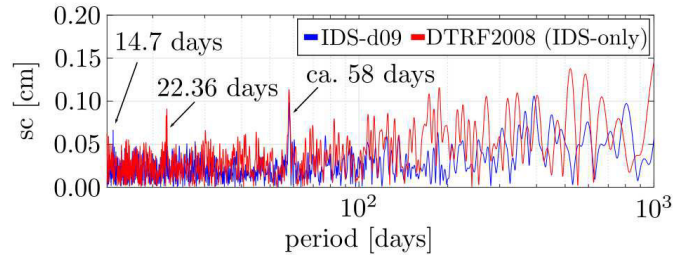


Figure 10: Spectra of both scale parameter time series shown in Fig. 10.

and Yellowknife (Canada, YELA) for the three coordinate components in north, east and height. In the north and east component of YASB, no annual peaks can be found. However, prominent spectral peaks at harmonics of the Jason-1/2 or TOPEX/Poseidon draconitic period can be clearly identified in both spectra with amplitudes of about 2.9 mm. The spectra of the height component of YASB contains only one peak of about 4.0 mm at 356.3 days which is near a multiple of the Jason/TOPEX draconitic period (117.32/117.83 days; see Tab. 1). The deviation of the peak from the draconitic multiple might be caused by annual variations due to the currently neglected NT-ATML corrections. Moreover, atmospheric loading, geocenter motion or mismodeling effects of sun-synchronous satellites can also cause annual signals in the station position time series (see also Section 4.1). The spectra of YELA are shown in Fig. 12. Again, the north and east component show no prominent annual signal but significant peaks at harmonics of the Jason/TOPEX draconitic period with amplitudes up to 5.5 mm. The height component contains a significant peak near the annual period with an amplitude of 5.0 mm and a peak at about 80 days with 5.0 mm amplitude.

Fig. 13 summarizes the histograms of the five largest significant peaks of each station for the north, east and height component. In all histograms, multiples of draconitic periods can be clearly identified. Especially the 58.7 day peak and the 117 day peak are visible in all components in about 10 % of the stations. The period of about 14 days is visible in about 28 % (north), 41 % (east) and 48 % (height) of the stations and might be related either to the IDS-d09 solution interval of 7 days or to tide model errors in the fortnightly frequency band (13.6, 14.2 and 14.8 days) as it is the case for GNSS products (Ray et al., 2013). In addition, Fig. 13 shows the amplitudes of the five largest significant peaks. In the horizontal components, the smallest amplitudes are larger than 1.0 mm whereas the height component amplitudes are at least 1.5 mm.

Tab. 4 summarizes the mean repeatability of the weekly DORIS position estimates of the IDS-d09 solution w.r.t. the DTRF2014 (IDS-only) solution. For comparison, the repeatability of the ITRF2005 and the ITRF2008 solution are shown (Angermann et al., 2010). Except in the east component, all components show a small improvement com-

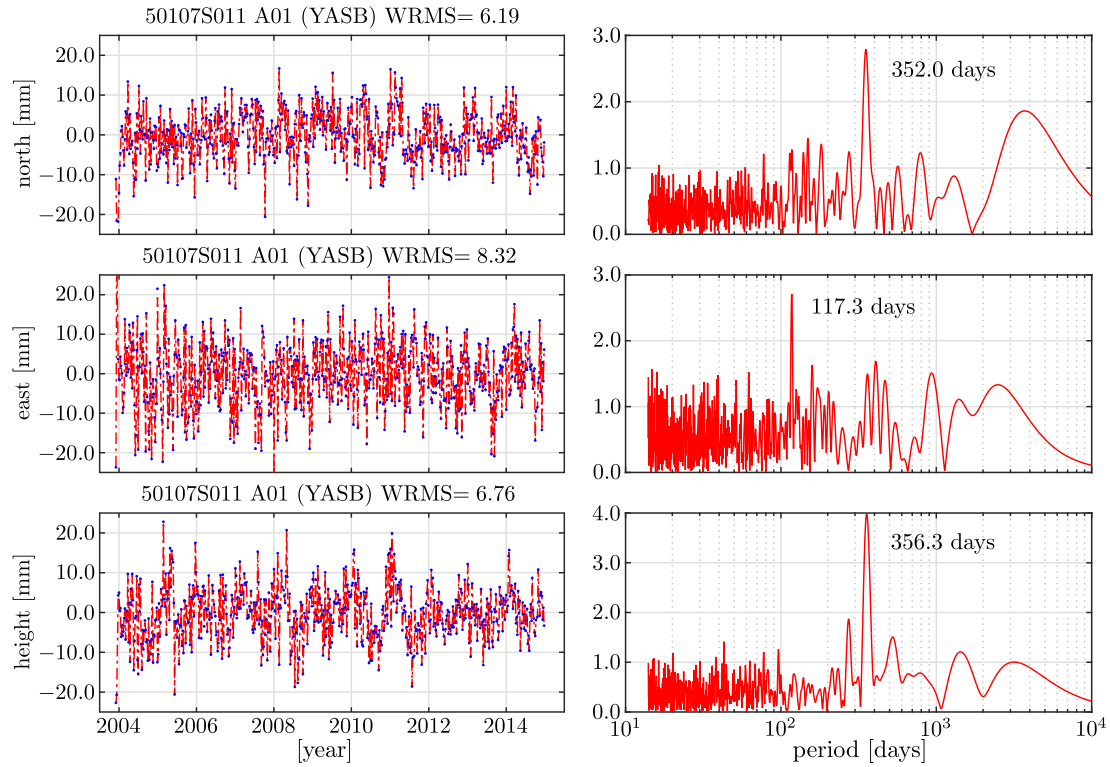


Figure 11: Time series (left plots) and spectra (right plots) of weekly station residuals of Yarragadee (Australia) in north, east and height. To compute a spectra of the time series, the non-equidistant station residuals (blue dots) are interpolated to an equally spaced (weekly) interval.

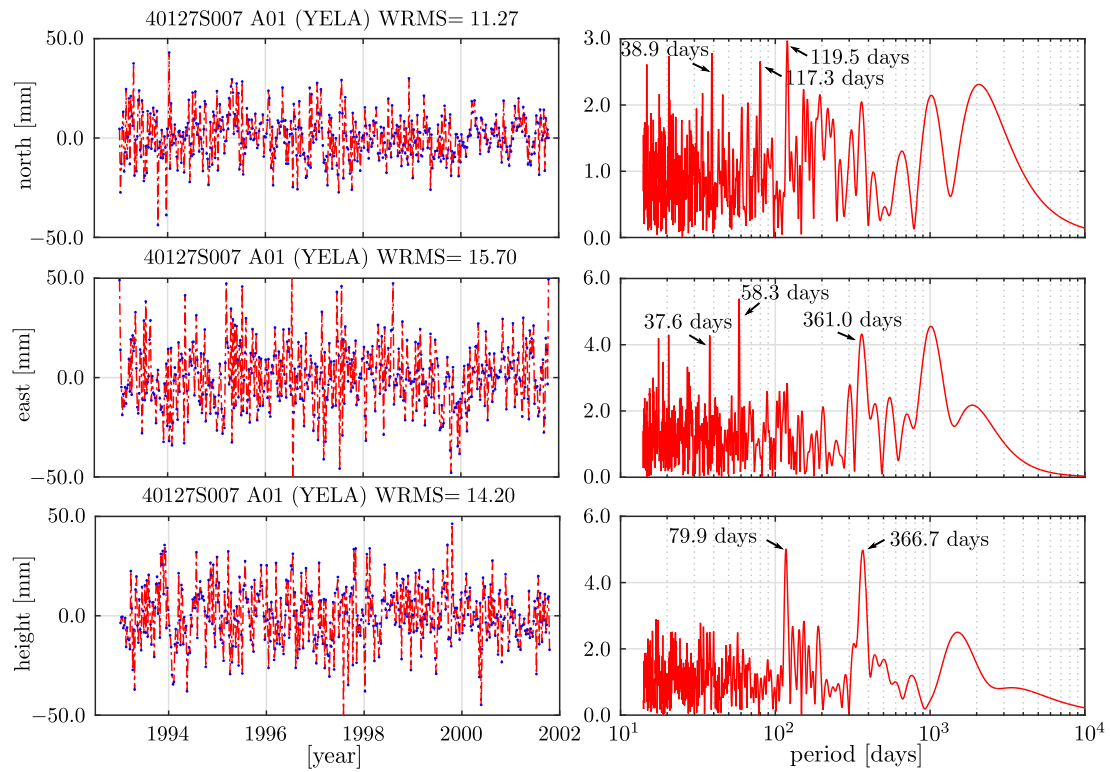


Figure 12: Time series (left plots) and spectra (right plots) of weekly station residuals of Yellowknife (Canada) in north, east and height. To compute a spectra of the time series, the non-equidistant station residuals (blue dots) are interpolated to an equally spaced (weekly) interval.

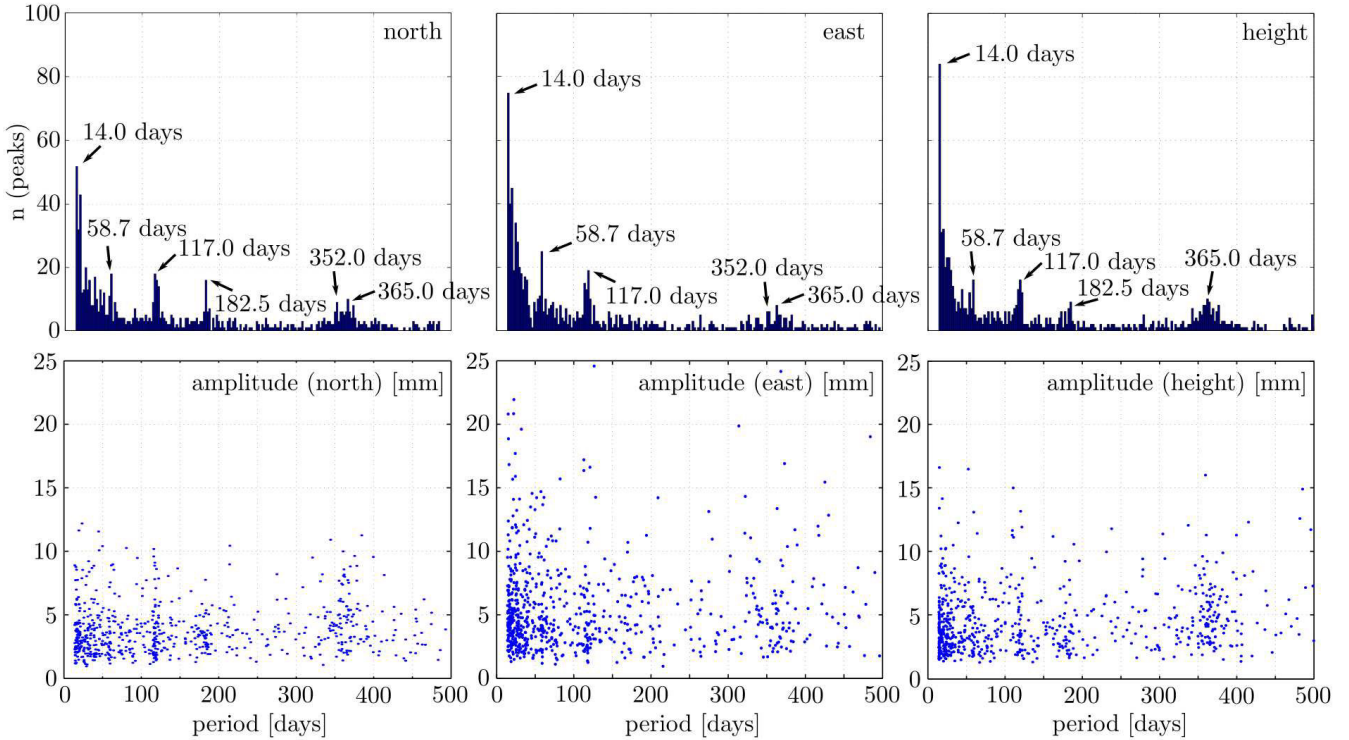


Figure 13: Upper three plots: histograms of the five largest significant peaks per station in north, east and height. Lower three plots: significant five largest amplitudes in north, east and height.

pared to the ITRF2008 solution. Especially the WRMS of the height component should be decreased compared to ITRF2008 since the new DGXX receivers allow to track beacons at low elevations (Moreaux et al., 2016).

Table 4: Mean station repeatability of weekly DORIS position estimates in north, east and height component w.r.t. DTRF2014 (IDS-only) solution. For a more detailed description of the ITRF2005 and ITRF2008 solution, see Angermann et al. (2010).

IDS solution	north [mm]	east [mm]	height [mm]
ITRF2005	24.3	32.3	22.5
ITRF2008	12.2	16.5	14.6
IDS-d09	11.6	17.9	13.9

4.2. IDS multi-year solution

The IDS multi-year solution is computed through accumulation the datum-free weekly NEQs and stacking common parameters like station coordinates and velocities (see Fig. 6). The realization of the geodetic datum is described in Sect. 3. The multi-year solution is validated w.r.t. DTRF2008 using a 14-parameter similarity transformation. The obtained transformation parameters (offsets and rates) are all below 1.0 mm which means that the datum definition (NNR-NNT-NNS constraints) worked correctly. The RMS values of the transformation are 7.3 mm for the station positions and 1.5 mm/yr for their velocities. These values are as twice as big as the RMS values of

the transformation of the DTRF2008 (IDS-only) solution w.r.t. the combined DTRF2008 (3.3 mm and 0.8 mm/yr; Seitz et al., 2012). A possible reason for these increased RMS values are the different network geometry due to changes in the modeling and due to newly introduced discontinuities. It is obvious, that both DTRF2008 solutions, which are based on the same input data, match better to each other than the IDS-d09 submission to the DTRF2008. For the transformation, the same 59 stations as for the datum realization have been used whereas for the DTRF2008 (IDS-only), only 45 stations have been used. If the transformation is performed with the 45 stations used for DTRF2008 (IDS-only), RMS values of 10.9 mm and 1.7 mm/yr are obtained. Fig. 14, 15 and 16 show the differences of the consistently adjusted terrestrial pole coordinates w.r.t. the IERS 08 C04 time series (<ftp://hpiers.obspm.fr/iers/eop/eopc04>), the formal errors of the differences and the corresponding spectra. The pole coordinates are adjusted consistently with the station coordinates and velocities. In the IDS combination, EOP of all AC solutions except the ESA and GOP solution are combined since the pole coordinates of the ESA solution show higher and more scattered differences w.r.t. IERS 08 C04 and the GOP polar coordinates comprise 14-day periods with high amplitudes (Moreaux et al., 2016). The x-component of the IDS-d09 pole coordinates shows a small drift and a larger scatter compared to the DTRF2008 solution (see Tab. 5). The y-component scatters slightly less than the DTRF2008 solution but shows

no drift at all. The larger scatter of the x-pole component might be, according to a discussion with the guest editor of this issue, related to some element of the processing at the fundamental level or how the data sets from the IDS ACs were handled. This effect needs some further discussion. The formal errors of both components are about two times larger compared to the DTRF2008 solution. This fact is caused by the incomplete SINEX files of the DTRF2008 solution. In these files, the statistical information was not included and the assumed stochastic values were too optimistic. This fact emphasizes the importance of reliable statistical information in the SINEX files (see Sect. 2). However, the impact of the different satellite constellations can be also identified in both formal error time series.

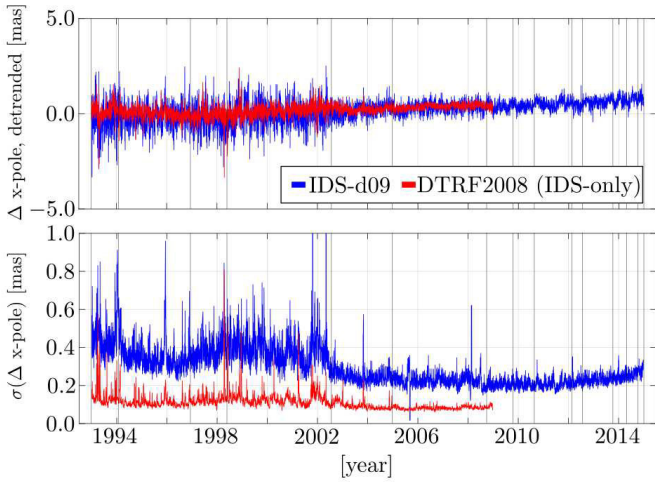


Figure 14: Upper plot: time series of x-pole differences of both IDS submissions (IDS-d09 and DTRF2008 (IDS-only)) w.r.t. IERS 08 C04. Lower plot: formal errors of differences.

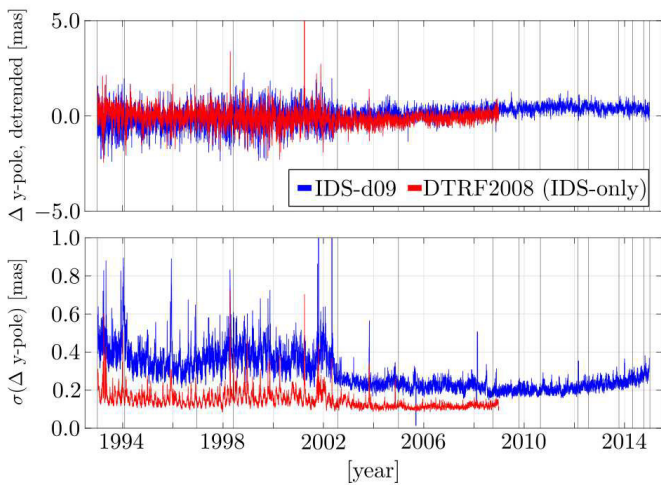


Figure 15: Upper plot: time series of y-pole differences of both IDS submissions (IDS-d09 and DTRF2008 (IDS-only)) w.r.t. IERS 08 C04. Lower plot: formal errors of differences.

Table 5: Weighted RMS values of the detrended pole coordinate time series of the IDS-d09 submission and the DTRF2008 (IDS-only) solution w.r.t. two reference time series. The values given in brackets are valid for the time interval between 1993.0 and 2009.0.

EOP	IDS-d09 w.r.t. IERS 08 C04 [mas]	DTRF2008 (IDS-only) w.r.t. IERS 05 C04 [mas]
x-pole	0.3620 (0.4053)	(0.2336)
y-pole	0.3124 (0.3407)	(0.3569)

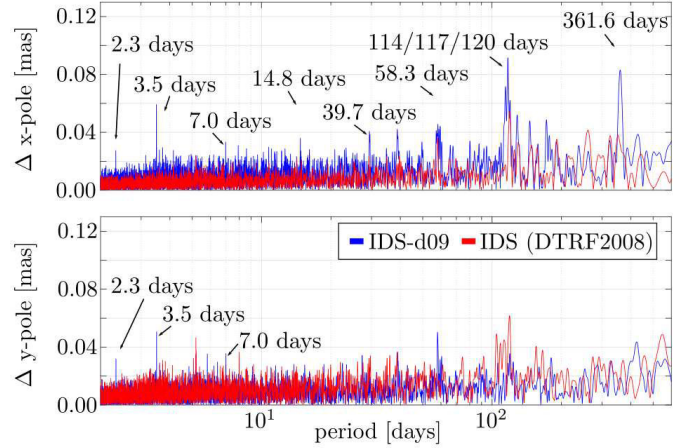


Figure 16: Spectra of pole coordinate differences shown in Fig. 14 and 15 w.r.t. IERS 08 C04.

Fig. 16 shows the spectra of the detrended difference time series of the obtained pole coordinates w.r.t. the IERS 08 C04 time series. Compared to the y-component, the x-component shows much more significant peaks at known periods. A possible reason for the peaks at 2.3, 3.5 and 7.0 days might be the arclengths of the individual IDS solutions (7.0 days: GSC, 3.5 days: LCA/GRG, 1.0 days: IGN, INA, GOP). The reason for the 14.8 day peak might be twofold: on the one hand, this systematic might be caused by the weekly combination interval of the IDS-d09 submissions. On the other hand, tide model errors in the fortnightly frequency band (e.g., 14.8 days is the M2 alias period caused by a 24 h sampling) might cause these systematic errors in the DORIS solutions since they are already identified in GNSS-derived polar motion (see also <http://acc.igs.org/erp-index.html>). The peaks at 39.7, 58.3 and around 117 days are multiples of the Jason/TOPEX draconitic periods. These peaks are significantly larger in the IDS-d09 than in the DTRF2008 differences. In the y-spectra, the 117 day period is totally damped in the IDS-d09 solution but the 58.3 day peaks is much more prominent than in the DTRF2008 solution. In addition to Fig. 16, Fig. 17 shows the spectra of the IDS-d09 pole coordinate time series divided into three different time periods. The upper panels show the spectra of the complete time series (1993.0 until 2015.0), the middle panels show the spectra of the TOPEX/Poseidon time

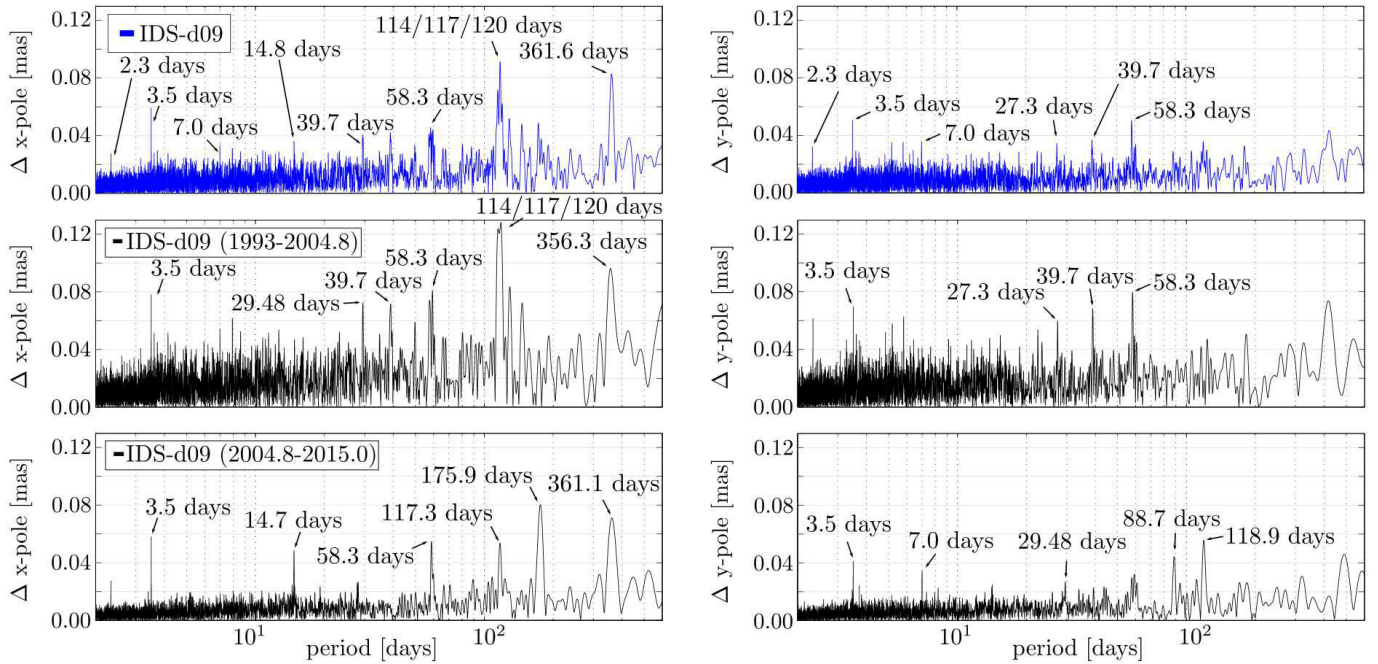


Figure 17: Spectra of pole coordinate differences shown in Fig. 14 and 15 w.r.t. IERS 08 C04, separated into complete time series (1993.0 until 2015.0; upper panels), TOPEX/Poseidon time period (1993.0 until 2004.8; middle panels) and Jason-1/2 time period (2004.8 until 2015.0, lower panels).

period (1993.0 until 2004.8) and the lower panels show the spectra of the Jason-1/2 time period (2004.8 until 2015.0). It can be clearly seen that the pole coordinates in the early years scatter much more than in the most recent years. The peaks at 58.3 and around 117 days in the TOPEX/Poseidon time period have nearly twice the amplitude as during the Jason-1/2 time period. In contrast to this, the 14.7 day peak solely occurs during the Jason-1/2 time period.

In summary, we can state that, in comparison with the DTRF2008 solution, the IDS-d09 solution shows more systematic errors at spurious draconitic harmonics and a larger scatter. This fact might be attributable to some IDS modeling and/or analysis and/or combination degradation.

5. Summary/Outlook

This paper evaluates the IDS-d09 submission to ITRF2014 and compares it with the IDS submission to ITRF2008. The submitted SINEX files are analyzed and different satellites used in the solutions and the weighting of the individual AC solutions are discussed. The squared sum of the residuals $\hat{\mathbf{v}}^T \mathbf{P} \hat{\mathbf{v}}$ is reconstructed from statistical information provided in the IDS SINEX files. The datum information of each SINEX file is evaluated and weekly datum-free normal equations are reconstructed.

The methodology of the combination of datum-free normal equations, which is used at DGF1-TUM in order to compute the DTRF2014, is briefly explained. Besides the multi-year solution, also weekly IDS-only solutions are

computed in order to identify discontinuities and systematics in the transformation parameters w.r.t. DTRF2008. For the DTRF2014, in total 56 discontinuities are introduced. A list of the discontinuities together with the reduction criteria and a list of the 15 reduced stations are also given in this paper.

The analysis of the weekly computed IDS-only solutions allows to assess the quality of the IDS submissions. Therefore, the most recent submission IDS-d09 is transformed to DTRF2008. The translation and scale parameter time series are compared to the parameter time series of the weekly DTRF2008 (IDS-only) solution. Systematics in the parameter time series can be allocated to changes in the DORIS satellite constellation. The spectra of the translation parameter time series confirm the high quality of the new IDS data since the scatter in the x- and y-translation is reduced compared to DTRF2008 (IDS-only). Also the annual amplitudes in the x- and y-component are reduced. Whereas the z-component of the DTRF2008 (IDS-only) translations contain signals near the annual frequency band, the IDS-d09 solution shows no peaks near that period. However, the z-component still shows a significant correlation with the Sunspot number. The scatter of all three IDS-d09 time series is reduced compared to DTRF2008 (IDS-only). The prominent drift which can be seen in the scale parameter time series of the DTRF2008 (IDS-only) data is totally removed in the new time series. Nevertheless, an offset in the scale time series after 2011.0 is visible. The spectra of the scale time series contains significant peaks at 14.7 days in case of IDS-d09 and 22.36 days in case of DTRF2008 (IDS-only). A prominent

peak at about 58 days (Jason-1/2 or TOPEX/Poseidon draconitic harmonic period) is slightly damped in the IDS-d09 time series.

In addition to the translation and scale parameter time series, also a time series of RMS values of the transformations is discussed. The IDS-d09 data shows in general higher RMS values which might be caused by some unidentified degradation in the IDS modeling, analysis and/or combination.

Besides the weekly transformation parameter time series, also the weekly transformation residuals per station are analyzed. As an example, the time series of Yarragadee (YASB) and Yellowknife (YELA) are shown. For YASB, only harmonics of draconitic periods of TOPEX/Poseidon and Jason-1/2 are visible in the spectra. The amplitudes are up to 2.9 mm in the horizontal components and 4.0 mm in the height component. For YELA, the height component contains a clear annual signal with 5.0 mm amplitude and a significant signal with a period of 80 days and an amplitude of 5.0 mm. This kind of analysis is done for all stations and the five most significant periods are summarized in histograms for the north, east and height component. Especially the 58.7 day and the 117 day period are visible in all components of about 10 % of all stations. A 14 day period is visible in about 28 % (north), 41 % (east) and 48 % (height) of all stations. Besides the spectral analysis of the station residuals, the analysis of the repeatability of the weekly position estimates allows to assess the internal accuracy of the IDS-d09 solutions. The mean repeatability is nearly the same for all station coordinate components (12.2 mm for north, 17.9 mm for east and 13.9 mm for height) and almost equal to the repeatability of the ITRF2008 IDS data.

The quality of the IDS multi-year solution is evaluated through a 14-parameter similarity transformation w.r.t. DTRF2008. All transformation parameters (offsets and rates) are smaller than 0.1 mm and 0.01 mm/yr which proves that the datum definition worked well. The RMS values of the transformation are twice as big as for the DTRF2008 (IDS-only) multi-year solution which might be caused by the same reason as for the weekly transformations (unidentified degradation in the IDS modeling).

Another focus is drawn on the consistently estimated EOP of the IDS multi-year solution. In order to assess their quality, differences w.r.t. IERS 08 C04 are computed. Several significant peaks at draconitic multiples of TOPEX/Poseidon and Jason-1/2, especially visible in IDS-d09, indicate problems with the solar radiation pressure or air drag modeling of these satellites. In the DTRF2008 (IDS-only) multi-year solution, these peaks are not clearly visible in the spectra. The formal errors of the pole parameters of the DTRF2008 (IDS-only) solution are much smaller than those of the IDS-d09 submission. This effect is caused by the too optimistic stochastic model of the DTRF2008 (IDS-only) solution due to not-booked statistical information in the submitted SINEX files. This fact underlines the importance of statistical information

provided by the technique-specific CCs. The impact of the different satellite constellations can be also identified in both formal error time series.

In summary, several improvements in the IDS analysis, new stations and new satellites result in a high quality IDS contribution to ITRF2014. This could be only achieved by the very high effort of the IDS in the last years (Willis et al., 2010, 2015; Moreaux et al., 2016). The quality of the IDS-d09 origin and scale is higher compared to the ITRF2008 data although this is not the case for the quality of station positions (higher transformation RMS) and polar motion (prominent draconitic harmonics in the spectra).

Acknowledgments

The authors want to thank the IDS community for the submitted high quality data for the ITRF2014 computation. Furthermore, special thanks are given to P. Willis who helped to improve the discontinuity list. The authors also thank the guest editor F. G. Lemoine of this issue and the three anonymous reviewers for their constructive comments on the manuscript.

References

- Altamimi Z., Collilieux X. Quality Assessment of the IDS Contribution to ITRF2008. *Adv Space Res* 45(12), pp 1500–1509, DOI: 10.1016/j.asr.2010.03.010, 2010
- Altamimi Z., Collilieux X., Métivier L. ITRF2008: an improved solution of the international terrestrial reference frame. *J Geod*, vol 85(8), pp 457–473, DOI: 10.1007/s00190-011-0444-4, 2011
- Altamimi Z. (2013) ITRF2013 call for participation, IERS message No. 225
- Angermann D., Seitz M., Drewes H. Analysis of the DORIS contributions to ITRF2008. *Adv Space Res* 46(12), pp 1633–1647, DOI: 10.1016/j.asr.2010.07.018, 2010
- Blewitt G., Lavallée D. Effect of annual signals on geodetic velocity. *J Geophys Res* 107(7), DOI:10.1029/2001JB000570, 2002
- Bloßfeld M. The key role of Satellite Laser Ranging towards the integrated estimation of geometry, rotation and gravitational field of the Earth. Dissertation, Technische Universität München, ISBN: 978-3-7696-5157-7, DGK Reihe C, Verlag der Bayerischen Akademie der Wissenschaften, URL: <http://dgk.badw.de/fileadmin/docs/c-745.pdf>, 2015
- Fagard H. Twenty years of evolution for the DORIS permanent network: from its initial deployment to its renovation. *J Geodesy*, vol. 80(8-11), pp 429–456, DOI: 10.1007/s00190-006-0084-2, 2006
- Gobindass M. L., Willis P., de Viron O., Sibthorpe A., Zelensky N. P., Ries J. C., Ferland R., Bay-Sever Y., Diamant M., Lemoine F. G. Improving DORIS geocenter time series using an empirical rescaling of solar radiation pressure models, *Adv Space Res* 44(11), pp 1279–1287, DOI: 10.1016/j.asr.2009.08.004, 2009
- Lemoine F. G., Chinn D. S., Zelensky N. P., Beall J. W., Le Bail K. The development of the GSFC DORIS contribution to ITRF2014, *Adv Space Res*, this issue, 2016.
- Moreaux G., Lemoine F. G., Capdeville H., Kuzin S., Otten M., Štěpánek P., Willis P., Ferrage P. IDS contribution to ITRF2014, *Adv Space Res*, this issue, 2016
- Ray J., Griffiths J., Collilieux X., Rebischung P. Subseasonal GNSS positioning errors. *Geophys Res Lett* 40(22), pp 5854–5860, DOI: 10.1002/2013GL058160, 2013
- Rudenko S., Dettmering D., Esselborn S., Schoene T., Foerste C., Lemoine J.-M., Ablain M., Alexandre D., Neumayer K.-H. Influence of time variable geopotential models on precise orbits of

altimetry satellites, global and regional mean sea level trends. *Adv Space Res* 54(1), pp 92–118, DOI: 10.1016/j.asr.2014.03.010, 2014

Schlax M. G., Chelton D. B. Aliased tidal errors in TOPEX/Poseidon sea surface height data, *J Geophys Res - Oceans* 99(C12), pp 24761–24774, DOI: 10.1029/94LC01925, 1994

Seitz M., Angermann D., Bloßfeld M., Drewes H., Gerstl M. The DGFI Realization of ITRS: DTRF2008. *J Geodesy*, vol 86(12), pp 1097–1123, DOI: 10.1007/s00190-012-0567-2, 2012

World Data Center SILSO. Sunspot Number and Long-term Solar Observations, Royal Observatory of Belgium, on-line Sunspot Number catalogue: <http://www.sidc.be/SILSO>, 1993–2015

Sillard P., Boucher C. A review of algebraic constraints in terrestrial reference frame datum definition. *J Geodesy*, vol 75(2-3), pp 63–73, DOI: 10.1007/s001900100166, 2001

Soudarin L., Capdeville H., Lemoine J.-M. Activity of the CNES/CLS Analysis Center for the IDS contribution to ITRF2014, *Adv Space Res*, this issue, 2016

Štěpánek P., Dousa J., Filler V. SPOT-5 DORIS oscillator instability due to South Atlantic Anomaly: mapping the effect and application of data corrective model. *Adv Space Res* 52(7), pp 1355–1365, DOI: 10.1016/j.asr.2013.07.010, 2014

Valette J. J., Lemoine F. G., Ferrage P., Yaya P., Altamimi Z., Willis P., Soudarin L. IDS Contribution to ITRF2008. *Adv Space Res* 46(12), pp 1614–1632, DOI: 10.1016/j.asr.2010.05.029, 2010

Willis P., Fagard H., Ferrage P., Lemoine F. G., Noll C. E., Noomen R., Otten M., Ries J. C., Rothacher M., Soudarin L., Tavernier G., Valette J.-J. The International DORIS Service (IDS): Toward maturity. *Adv Space Res* 45(12), pp 1408–1420, DOI: 10.1016/j.asr.2009.11.018, 2010

Willis P., Lemoine F. G., Soudarin L., Moreaux G., Soudarin L., Ferrage P., Ries J., Otten M., Saunier J., Noll C., Biancale R., Luzum B. The International DORIS Service (IDS): Recent developments in preparation for ITRF2013. *IAG Symposia Series*, vol 143, pp 1–9, DOI: 10.1007/1345_2015_164, 2015